Received: 12 December 2020 | Revised: 13 February 2021 | Accepted: 3 March 2021

IET Radar, Sonar & Navigation

DOI: 10.1049/rsn2.12091

The Institution of Engineering and Technology WILEY

ORIGINAL RESEARCH PAPER

Real-time capable multiple-input–multiple-output SONAR systems—An algorithmic approach

Thorben Kaak[1] | **Jan Abshagen**[2] | **Gerhard Schmidt**[1]

[1]Digital Signal Processing and System Theory, Kiel University, Kiel, Germany

[2]Maritime Technology and Research (WTD 71), Bundeswehr Technical Center for Ships and Naval Weapons, Kiel, Germany

Correspondence

Gerhard Schmidt, Digital Signal Processing and System Theory, Kiel University, Kaiserstr. 2, 24143 Kiel, Germany.
Email: gus@tf.uni-kiel.de

Abstract

In recent years, significant effort has been allocated to research on multiple-input–multiple-output (MIMO) sound navigation and ranging (SONAR) and RADAR systems. Most work has been conducted on the general theoretical functionality of such systems. Less effort has been applied to considerations of the real-time MIMO capability, although this is an important factor for the application of these new algorithms in real SONAR systems. To account for this, the following work focusses, after introducing the used methodology and revisiting the general MIMO idea and considered system, on more effective permutations of the involved algorithms in the reduction of floating-point operations. In this context, the general necessity of the algorithms utilized is shown. Furthermore, it is proven that the reduction in computational load does not affect the performance of the system. In addition, the main algorithmic parts of MIMO systems can be exchanged almost arbitrarily under given restrictions without changing the result. Therefore, the performance differences in floating-point operations are depicted to give an estimate of the achievable degree of complexity reduction. The results for the investigated systems and algorithms are obtained by applying a system simulation of a simple underwater channel. The obtained results were also verified using a real MIMO SONAR system operating in real time.

1 | INTRODUCTION

Good performance of sound navigation and ranging (SONAR) systems in environments with a strong reverberation and low signal-to-noise ratio (SNR) is an important indicator for a powerful system. The application of multiple-input multiple-output (MIMO) techniques is a promising approach to increase performance for crucial scenarios and has been theoretically discussed in numerous publications [1–5].

Interest in MIMO RADAR (radio detection and ranging) first developed in the early 2000s—for example, in [6]. At that time, merely theoretical considerations were made. In the following years, research results on practical applications were obtained, and interest by the SONAR community increased [4, 7]. Nevertheless, research on the practical feasibility was missing in the past because the required hardware for MIMO SONAR systems was not available (mainly by means of appropriate projector arrays). This shortage has now been overcome by *WTD 71* and the chair of *Digital Signal Processing and System Theory* at Kiel University by acquiring appropriate hardware from *Atlas Elektronik* (Figure 1 depicts these MIMO transmit arrays) and paving the way for practical applications of the promising MIMO technique.

Some of the previously investigated advantages of MIMO processing include the highly improved angular resolution, a perfect steering in the same direction of transmit and receive beamformer as both are calculated at receive side, and as a consequence, improved performance of localization and detection of targets [4]. Those theoretical benefits will not be investigated further in this contribution but motivate a discussion of the necessity of a reduction in computational complexity to take full advantage of the MIMO principle for real-world SONAR applications.

In standard MIMO applications, mutually orthogonal signals are utilized for the different transmit elements to achieve the before-mentioned benefits of MIMO technology in RADAR or SONAR applications. One can also utilize these properties to generate signals that are mutually orthogonal

FIGURE 1 Projector array. Two staves with 16 projectors within each stave can be used for MIMO measurements in the future. Each projector can be driven with an individual signal

between different pings, thus defining a sequence of signal groups. Given a capable hardware and channel as well as appropriate signal design, the ping period of the system can be redefined.

This new concept paired with frame-based processing as discussed in Section 4 enables the SONAR system to process and react to incoming signals much faster—unfortunately and obviously at the cost of higher computational complexity. This again emphasizes the necessity of effective (in terms of computational complexity) algorithms to retain the real-time capability of the underlying SONAR system.

An additional scope of MIMO is the application to synthetic aperture SONAR where the processing time of the system, and such the expense for measurement trials, can be highly reduced.

The application of MIMO techniques known from communication theory as well as the general system model have been introduced by Rabideau and Parker [1], Bliss and Forsythe [3], and Bekkerman and Tabrikian [4] and will not be reviewed in this contribution. In Section 2, the necessary algorithms for a SONAR processing are given, and possible permutations of the algorithms in the processing sequence are suggested.

A combined matched filter and transmit beamformer approach is presented in Section 3 to counteract the increase of computational load. The concept of virtual arrays and co-arrays as well as their differences and advantages have been investigated by [8–11] and are hereby presumed in this publication. Investigations concerning the real-time capability for the different approaches presented—including the combined matched filter—for SIMO (single-input multiple-output) are done in Section 4. This is followed by a comparison of simulations (Section 5). Finally, the paper is concluded, and the outlook for future work is given.

2 | MULTIPLE-INPUT–MULTIPLE-OUTPUT SYSTEM PROCESSING CHAIN

To understand the idea behind the MIMO matched filter algorithm presented here and considerations regarding the real-time capability of SONAR systems, the underlying processing chain is outlined. We will focus only on basic versions of the required algorithmic parts—extensions to more sophisticated approaches, however, are possible in a straightforward manner. The results in terms of reduction in computational load are usually even greater for the extended approaches.

The output signals of the receive beamforming are denoted by subscript $\_{\mathrm{Rx}}$ in the following, while those of receive side transmit beamforming are denoted by $\_{\mathrm{Tx}}$. The time domain signals are depicted by small letters with square brackets and the frequency domain signals by capital letters with curved brackets. If the beamformed signal is based on a matched filtered signal, the signal is depicted by letter $z\_[n]$ or $Z\_(\mu)$ and otherwise by $y\_[n]$ or $Y\_(\mu)$ (vectors and matrices are denoted by bold characters).

Before the algorithms for MIMO and SIMO are compared, their respective naming is briefly clarified. Generally, the terms *single input (SI)*, *multiple-input (MI)*, and *multiple-output (MO)* are defined within the channel through which a signal is transferred. In the case of SIMO, one or several non-orthogonal transmit signals are transmitted into the channel. No matter where in the channel a probing signal is taken from, one records the superposition of the individual transmit signals. As they are not orthogonal, they cannot be separated properly any more, and hence, it can be seen as an SI to the channel. For MIMO where orthogonal signals are transmitted, the superposition of the individual signals can be reverted and assigned to their transmit channels identically to MIs.

The use of the terminology single and multiple is thus based on the assignability of the transmitted signals (at the receive side) to the transmission elements. To be more precise, the assignability of the signals to the elements must in general be possible. Thus, this can be applied to the receive side as well. If there is more than one receive element, *MOs* are taken from the channel, which is done for both SIMO and MIMO. This property leads to a major advantage of MIMO over SIMO, namely, the shift of the transmit beamforming algorithm to the receive side, and thus, a great gain in flexibility and general performance (see Section 2.2.2) can be achieved. Nevertheless, this advantage comes with a price—a lower SNR than that of SIMO, where the transmitted energy is concentrated in a defined direction.

A SONAR system is also classified on the basis of the positioning of the transmitting and receiving elements and the individual elements in general. On this basis, SONAR systems are divided into monostatic (transmitter and receiver at almost the same position), bistatic (transmitter and receiver separated), and multistatic (in addition to bistatic systems, the individual transmitter and receiver elements or subarrays are separated locally as well) systems. For the algorithms presented that follow, a monostatic active SONAR system is assumed.

2.1 | Transmit processing

Transmit processing in the case of MIMO can be less complex than SIMO systems because the step of transmit beamforming is neglected (for non-hybrid systems) because of the necessity of transmitting ideally perfect orthogonal sequences. Because

of this no beam lobe is pronounced, and as such no steering is possible. Other than that, the transmit processing can be seen to be identical to SIMO.

Furthermore, each transmitter and receiver is, for the sake of simplicity, assumed to have omnidirectional characteristics. They are additionally assumed to be utilized at optimal power, and no mutual phase shifts are introduced.

Additionally, shadowing effects based on the array geometries need to be considered in a real system but are neglected in the following if not otherwise stated. For this very simplified system, the transmit processing reduces to a simple mapping of the transmit signals to output channels (i.e. transducers).

In addition, hybrid approaches with a mixture of mutual orthogonal and non-orthogonal signals have been proposed, for example, in [12, 13]. For these approaches, the relations presented in the paper change, and while an adaption is possible in most cases, some changes need to be made that are not considered here. In addition to the transmit processing, the receive processing would need to be adapted as well.

2.2 | Multiple-input multiple-output receive processing

Most of the processing of this simplified system is shifted to the receive side. The most basic and additionally most important algorithms utilized in MIMO receive processing are the matched filter and beamformer. Their basic structure is presented in the subsequent sections to prepare the reader for the concept of the MIMO matched filter and the corresponding considerations of computational complexity.

2.2.1 | Matched filter

Being a crucial part of MIMO signal processing, the general idea of a matched filter, including assumptions and simplifications made for the consideration of MIMO systems, will be presented in the following. The general aim of a matched filter is to maximize the SNR. Under the assumption of available noise distortions being white, its functionality is based on the convolution of the signal under test with a time-reversed prototype signal (here: transmit signal). The (weighted) convolution of two discrete signals $x[n]$ and $y[-n]$ is related to the correlation at delay $\kappa \in \mathbb{Z}$ by

$$\begin{aligned} R_{xy}[\kappa] &= \mathrm{E}\{x^*[n]\, y[n+\kappa]\} \\ &\approx \frac{1}{N}\sum_{n=0}^{N-1} x^*[n]\, y[\kappa+n] = \widehat{R}_{xy}[\kappa], \end{aligned} \tag{1}$$

with $E\{...\}$ denoting the expectation operator, and the matched filter is treated with this notation.

The analog-to-digital (AD)-converted discrete input signal of the l-th channel of the SONAR system is denoted by $y_l[n] \in \mathbb{R}$, with $n \in \mathbb{Z}$ as the discrete time index. The discrete signal for the m-th transmit channel—before the digital-to-analogue converter—is defined as $x_m[n] \in \mathbb{R}$. Furthermore, let the indices denoting the l-th receiver and m-th transmitter element take values from $l \in \{0, 1, \ldots, N_{\mathrm{Rx}} - 1\}$ and $m \in \{0, 1, \ldots, N_{Tx} - 1\}$, respectively. Both signals are normalized such that the following holds:

$$\left|y_l[n]\right| \le 1 \ \wedge \ \left|x_m[n]\right| \le 1 \quad \forall\, n \in \mathbb{Z}, \tag{2}$$

Additionally, the signal processing starts at $n = 0$:

$$y_l[n] = 0 \ \wedge \ x_m[n] = 0 \quad \forall\, n < 0. \tag{3}$$

Let the estimate of the cross-correlation between two channels i and j for cutting out vectors of length N_i and N_j of transmit signals $x_i[n]$ and $x_j[n]$ respectively with be defined by

$$\widehat{R}_{x_i,x_j}[\kappa] = \frac{1}{\min\{N_i,\, N_j - \kappa\}} \sum_{n=0}^{\min\{N_i,\, N_j-\kappa\}-1} x_i^*[n]\, x_j[n+\kappa]. \tag{4}$$

For this definition, κ is restricted such that the following holds:

$$\kappa \in \{-(N_j - 1), \ldots, N_i - 1\} \subseteq \mathbb{Z} \tag{5}$$

For an ideal MIMO system, which is assumed in the following (if not further noted), the signals are designed such that they are perfectly mutually orthogonal (for $i \neq j$). The individual channel pairs of Equation 4 can be combined in a matrix with $\mathbb{R}^{N_{\mathrm{Tx}} \times N_{\mathrm{Tx}}}$ as

$$\widehat{\boldsymbol{R}}_{\boldsymbol{xx}}[\kappa] = \begin{bmatrix} \widehat{R}_{x_0,x_0}[\kappa] & \cdots & \widehat{R}_{x_0,x_{N_{\mathrm{Tx}}-1}}[\kappa] \\ \widehat{R}_{x_1,x_0}[\kappa] & \cdots & \widehat{R}_{x_1,x_{N_{\mathrm{Tx}}-1}}[\kappa] \\ \vdots & \ddots & \vdots \\ \widehat{R}_{x_{N_{\mathrm{Tx}}-1},x_0}[\kappa] & \cdots & \widehat{R}_{x_{N_{\mathrm{Tx}}-1},x_{N_{\mathrm{Tx}}-1}}[\kappa] \end{bmatrix}. \tag{6}$$

Because of mutually orthogonal transmit signals, the following relation holds as well for $\sigma_{x_i}^2$ depicting the power of the signal $x_i[n]$:

$$\max_{\kappa}\left\{\left|\widehat{R}_{x_i,x_j}[\kappa]\right|\right\} = \begin{cases} \sigma_{x_i}^2 \le 1, & \text{for } i = j \\ 0, & \text{else} \end{cases}. \tag{7}$$

Here, we assume that the means of all transmit signals are zero. This property is now exploited in the matched filter of an active SONAR systems processing chain, which should not match to just one transmit signal but N_{Tx}. This is achieved by

the computation of N_{Tx} matched filters in parallel. To be more precise, the matching to the N_{Tx} transmit signals is done for all N_{Rx} receive signals and can be described by

$$z_{l,m}[\kappa] = \widehat{R}_{y_l,x_m}[\kappa] \tag{8}$$

and

$$\boldsymbol{\zeta}[\kappa] = \begin{bmatrix} z_{0,0}[\kappa] & \cdots & z_{0,N_{\mathrm{Tx}}-1}[\kappa] \\ z_{1,0}[\kappa] & \cdots & z_{1,N_{\mathrm{Tx}}-1}[\kappa] \\ \vdots & \ddots & \vdots \\ z_{N_{\mathrm{Rx}}-1,0}[\kappa] & \cdots & z_{N_{\mathrm{Rx}}-1,N_{\mathrm{Tx}}-1}[\kappa] \end{bmatrix}. \tag{9}$$

$\boldsymbol{\zeta}[\kappa]$ with dimension $N_{\mathrm{Rx}} \times N_{\mathrm{Tx}}$ describes the $N_{\mathrm{tot}} = N_{\mathrm{Rx}} \cdot N_{\mathrm{Tx}}$ outputs of the matched filters. Due to the assumption of mutually orthogonal signals, the path of just one transmitter–receiver pair is preserved per correlation output; see Equation (7). This is finally used in an extended receive beamforming unit.

In our system, the matched filtering is realized in the frequency domain as the correlation becomes a multiplication, and as such, the computational load is reduced. The frequency domain signal is depicted by $Z(\mu)$ where $\mu \in \{0, 1, \ldots, N_{\mathrm{FFT}} - 1\}$.

2.2.2 | Beamforming

To be able to follow the application of an extended beamforming, the idea of the basic beamformer is first repeated in the following. The application of receive side beamforming is another crucial step in SONAR processing in obtaining an estimate of the target's angular position. The general idea of beamforming is the time-wise alignment of receive (and/or transmit) signals according to the array geometry and hypothesis of the target's angular position to achieve a constructive superposition of the individual signals, and hence, an increase in SNR.

To understand the benefits of MIMO over SIMO and the interchangeability of certain algorithms, a simple consideration of the delays introduced to the transmit signal when travelling through the channel to the receive element must be performed. Any influence of noise or attenuation of the original signal is neglected in the following, as for this proceeding, a basic idea of the general process of beamforming is sufficient to motivate the principles of a MIMO matched filter. For a more in-depth derivation based on a more detailed channel model, the reader is referred to, for example, [4].

Given a target $p \in \{0, 1, \ldots, P-1\}$ with $P \in \mathbb{N}$ in direction $\theta_{\mathrm{Tx},p}$ at distance $r_{\mathrm{Tx},p}$ relative to the centre of the transmitter array and in direction $\theta_{\mathrm{Rx},p}$ at distance $r_{\mathrm{Rx},p}$ relative to the centre of the receiver array, the transmit signal of array element m is delayed by

$$\kappa_{m,p,l} = \kappa_{m,p} + \kappa_{p,l}, \tag{10}$$

when reaching the l-th receive element. $\kappa_{m,p}$ describes the delay introduced to the transmit signal by travelling from transmitter m to target p and $\kappa_{p,l}$ the delay for travelling from target p to receiver l. The model is further simplified by assuming a monostatic setup (i.e. transmitter and receiver are *colocated*—they are located at the same place). Hence, we have

$$\theta_p = \theta_{\mathrm{Tx},p} \approx \theta_{\mathrm{Rx},p} \quad \text{and} \tag{11}$$

$$r_p = r_{\mathrm{Tx},p} \approx r_{\mathrm{Rx},p}. \tag{12}$$

Without loss of generality, the mutual delay proportional to the target's range r_p can be neglected. Following these simplifications, the delays at certain elements solely depend on the target's angle relative to the arrays (θ_p) and are denoted by $\widetilde{\kappa}_{m,p}$ and $\widetilde{\kappa}_{p,l}$ for transmit and receive array elements, respectively.

Receive side beamforming can now be performed either separately for the delays $\widetilde{\kappa}_{m,p}$ and $\widetilde{\kappa}_{p,l}$—regardless of the different permutations of the algorithms in the processing sequence—or in a combined manner for $\widetilde{\kappa}_{m,p,l} = \widetilde{\kappa}_{m,p} + \widetilde{\kappa}_{p,l}$ given separated coherent signals (e.g. because of matched filtering as described in the previous section). Because of this, it is obvious that there are at least three possible realizations in the permutation of the system's subalgorithms. In fact, there are more than three realizations, as will be shown in Section 2.3.

These possibilities yield an improved 'offline' beamforming, as the transmit beam can be performed in a *post-ping* manner, and additionally, the transmit and receive beamformers are always steering in exactly the same direction, and hence, missteering is prevented, and as a consequence, an unwanted attenuation is averted. A derivation for the weights of the beamformers is omitted at this point; reference should again be made to existing literature—for example, [4, 5, 8].

Additionally, it should be noted that given a noise assumed to be uncorrelated to the transmitted signal, the SNR improvement due to beamforming depends on the permutation of the algorithms in the processing sequence. This leads to a superior processing output for those permutations where the receive beamforming is done previous to the matched filtering. For a fair comparison of MIMO and SIMO processing, this needs to be considered, and as well, this introduces a drawback of MIMO but should nevertheless be omitted at this point, as it is focussed on a real-time capability of a MIMO SONAR system, and as it will be seen later, the most promising permutation of the subalgorithms overcomes this drawback.

2.3 | Possible realizations

The previously introduced algorithms are now used to build up a MIMO processing chain referred to as *preprocessing* in the following. The term *postprocessing* implies algorithms like detection and tracking, which are not further considered here. The biggest difference of MIMO compared with SIMO is the

availability of receive side transmit beamforming and the processing of N_{Tx} parallel matched filters. The beforementioned possibility of interchanging the order of several subalgorithms while keeping the output signals just holds for time invariant filters, which is true under the given assumptions.

Furthermore, the matched filtering is necessary previous to transmit beamforming. Otherwise, a constructive superposition of the signals is not possible. Obviously, the following permutations are possible:

(a) Receive bf. | matched filtering | transmit bf,
(b) Matched filtering | receive bf. | transmit bf,
(c) Matched filtering | transmit bf. | receive bf,
(d) Matched filtering | combined receive/transmit bf..

In addition, the integration of the transmit beamforming into the matched filtering process is possible and yields some important advantages in the sense of computational complexity. This new structure is proposed in the next section. Please note that the amount of parallel processed matched filters changes to the number of beams processed (N_{B}) such that the list above can be extended:

(e) *MIMO matched filtering* | receive bf. and
(f) Receive bf. | *MIMO matched filtering*.

The general receive side processing is shown in the upper part of Figure 2, while the depicted permutations of the algorithms in the processing sequence are sketched in the lower part of Figure 2. A parallel processing of algorithms is depicted by stacking of the module blocks. This is additionally visualized by parallel arrows. Moreover, the dimension of the dataflow is depicted beneath the arrows. This type of representation alone gives a good overview of the computational effort required for the individual implementations. This will be discussed in detail in Section 4. It should be anticipated at this point that the proposed MIMO structures (e) and (f) drastically reduce the computational load compared with direct MIMO realizations (a) to (d) of the algorithms (details on this will be given in the next sections).

MIMO processing will later be compared with classic SIMO processing. For this purpose, the following signal processing chains are defined as well:

(i) SIMO: Receive bf. | matched filtering and
(ii) SIMO: Matched filtering | receive bf.

The matched filtering in the SIMO case is done for just one signal, as the same time-shifted version of a signal is transmitted at all elements. The receive beamformer is identical to that of the MIMO algorithms. It should be noted that in the case of SIMO, several transmit beams, and therefore multiple pings, must be sent out to cover an identical area in a similar way as in the case with MIMO. This will also be considered later.

3 | MULTIPLE-INPUT MULTIPLE-OUTPUT MATCHED FILTER

In classic (SIMO) SONAR or RADAR applications, the matched filtering process is executed for a single transmit signal to increase the SNR. For the direct application to MIMO systems, this leads to the processing of N_{Tx} matched filters in parallel to harness the newly emerged degrees of freedom. Those output signals are then input to a beamforming process as described in Section 2.2.

Our newly proposed technique incorporates at least the receive side transmit beamforming into the matched filtering process. Therefore, a new prototype signal $\widetilde{x}[n,\theta] \in \mathbb{C}$ with incident angle θ is introduced, which is calculated as the sum of the delayed original orthogonal signals:

$$\widetilde{x}[n,\theta] = \sum_{l=0}^{N_{\mathrm{Tx}}-1} x_l[n, -\varkappa_l(\theta)]. \tag{13}$$

The delay $\varkappa_l(\theta)$ is calculated according to the array geometry and the position of transmit element l. Note that $\varkappa_l(\theta) \in \mathbb{R}$ describes a non-integer delay of a discrete time domain signal. For a uniform linear array (ULA), it is given by

$$\varkappa_l(\theta) = \left(l - \frac{N_{\mathrm{Tx}}-1}{2}\right) \frac{d_{\mathrm{El,Tx}} \sin\theta}{c_{\mathrm{w}}} \frac{1}{f_{\mathrm{s}}}. \tag{14}$$

The term c_{w} describes the sound velocity in water, f_{s} the system's sample rate, $d_{\mathrm{El,Tx}}$ the distance between two consecutive transmitter elements, and $x_l[n, -\varkappa_l(\theta)] \in \mathbb{C}$ describes a complex signal at transmitter element l delayed in dependence of the hypothetical transmit angle by $\varkappa_l(\theta)$. As an example, for narrowband signals this can be calculated as follows:

$$x_l[n, -\varkappa_l(\theta)] = x_l[n - \lfloor \varkappa_l(\theta) \rfloor]\, e^{j2\pi f (\varkappa_l(\theta) - \lfloor \varkappa_l(\theta) \rfloor) \frac{1}{f_{\mathrm{s}}}}. \tag{15}$$

where f describes the narrowband signal (centre) frequency. Due to the matching to $\widetilde{x}[n,\theta]$, which equals the output of a transmit beamformer pointing in direction θ, signals from a specific direction are strengthened while those from other directions are attenuated. Hence, the transmit beamforming is incorporated into the matched filtering process. Please note that more complex beamformer algorithms can also be applied here without losing the advantages in terms of computational complexity and will be described next.

Following this implementation, the number of matched filter prototype signals changes from N_{Tx} to N_{B} (number of beams calculated), and depending on the permutation of the algorithms, the filtering number of for each filter changes from N_{B} (for processing chain (a)) or N_{Rx} (for (b)/(c)/(d)) to either N_{Rx} (for MIMO processing (e) or 1 for (f)).

As will be shown in the next section, case (f) especially outperforms the straightforward application of MIMO

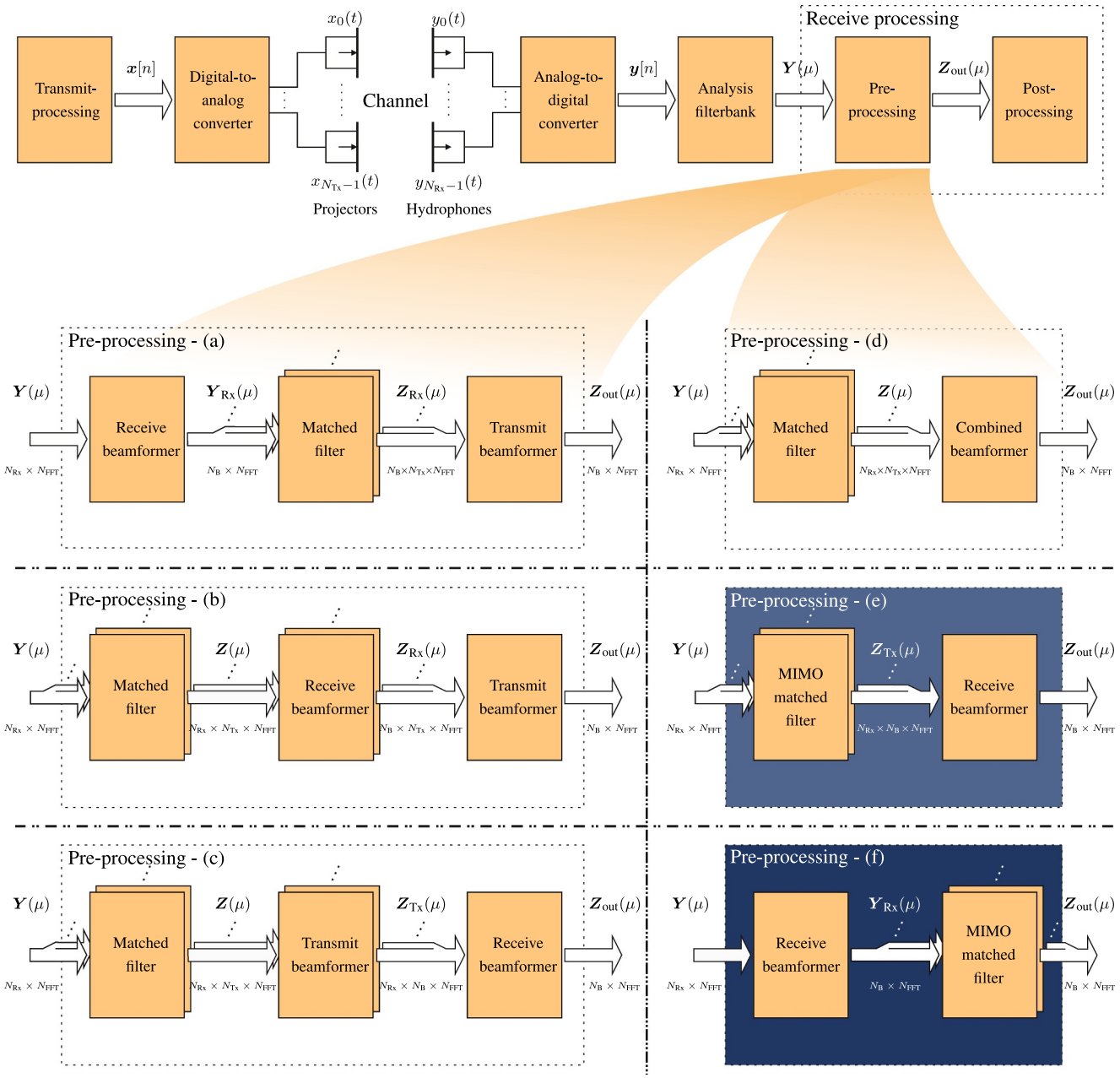

FIGURE 2 Preprocessing permutations as introduced in Section 2 and corresponding dimensions for inputs and outputs of subalgorithms. Vectors are depicted by bold letters. Time domain signals are depicted by time index *n* and square brackets (e.g. ***x[n]*** is time domain vector). Frequency domain quantities are depicted by capitals and frequency index μ in curved brackets (e.g. ***Z(μ)***). Our newly introduced signal processing structures—superior in terms of computing power—are highlighted in blue

algorithmic in terms of reduction of computational complexity, and because of this, also for a possible real-time-capable SONAR system. In parallel with this, some rules are introduced to achieve a fair comparison between the different realizations for MIMO processing chains.

4 | REAL-TIME CAPABILITY

A closer look at the different MIMO realizations shown in Figure 2 reveals the following observations regarding computational complexity. When looking at variant (a), it becomes clear that only the matched filter has to be computed several times (here N_B). This is generally necessary for each variant because the correlation is either performed with the different orthogonal signals (variants (a)–(d)), or in the case of the MIMO matched filter (variants (e) and (f)), with a directional sum signal. In the case of variants (b) and (c), in addition to an N_{Rx} parallel calculation of the matched filters, the receive and transmit beamforming must also be calculated N_{Tx} and N_{Rx} times, respectively, in parallel. The downstream beamformers (transmit and receive beamforming, respectively) are

already supplied with direction-dependent data. Thus, the complexity is further reduced because the second beamforming is performed only for the already specified directions. For variant (d), in contrast to the previous discussion, a combined beamformer with $N_{\mathrm{Tx}} \times N_{\mathrm{Rx}}$ elements will be computed. The complexity because the matched filter is also upstream is thus at a similar level to that of (b) and (c). The two algorithms with the presented MIMO matched filter (e) and (f) differ mainly in the number of matched filters that must be computed. In the case of (e), all N_{B} prototype signals are filtered for all N_{Rx} receive elements and receive beamformed signals afterwards. In the case of (f), on the other hand, the directions are already specified by the upstream receive beamformer, which means that only matched filters must be calculated—each direction is filtered with the corresponding direction-dependent prototype signal. This explains the even higher efficiency of (f).

After the definition of the processing structure and the general behaviour of a MIMO system, two general processing approaches are possible (See Figure 3):

(1) Ping-based processing, which is often used in RADAR or SONAR applications (i.e. the data of one ping is collected and processed en bloc) and

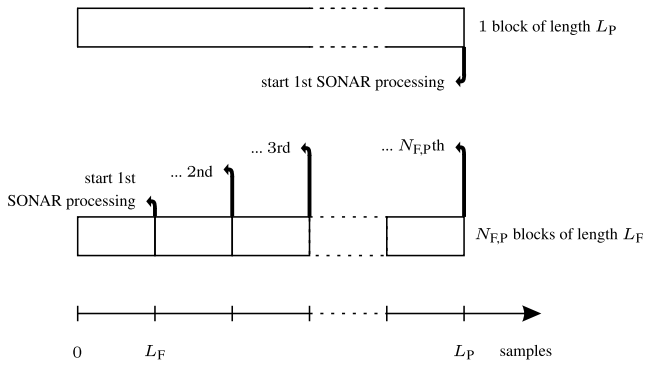

FIGURE 3 Comparison of the temporal processing sequence for ping-based and frame-based processing

(2) Frame-based methods, which are common practice for real-time audio signal processing. With frame-based processing, the block size is usually much smaller than the ping duration. This results in the entire processing chain being run multiple times within one ping. This more frequent computation with smaller amounts of data in turn leads to greater flexibility in the algorithms utilized (as explained later). A more detailed explanation of how frame-based processing is utilized in SONAR systems can be found, for example, in [14].

In the latter, the real-time capability of a more or less standard MIMO approach is examined, where orthogonal signals are utilized for the different transmit elements to achieve enhanced processing.

The system's real-time capability is compared for both realizations (ping-based and frame-based processing). To initially reduce the computational complexity—independent of the processing approaches—the hydrophone input data of the underlying system is blockwise-transformed into the frequency domain, and the processing is done herein.

As mentioned before, the concept of frame-based processing can be extended by utilizing the crucial MIMO properties to generate signals that are mutually orthogonal between different pings, thus defining a sequence of signal groups. Given capable hardware and appropriate signal design, the ping period of the system can be redefined. The conventional ping period T_{p} now refers to the duration of the sequence of N_{MP} signal groups, whereas $T_{\mathrm{P,MP}} = T_{\mathrm{p}}/N_{\mathrm{MP}}$ yields the effective ping period. This new ping period defines the refresh-rate of the SONAR plots and with $T_{\mathrm{P,MP}} \leq T_{\mathrm{p}}$ enhances the temporal resolution. Because of the reduced correlation over different ping periods, improvements in the localization and detection process of targets are possible. The general idea is depicted in Figure 4.

To understand the motivation behind the following considerations, our basic setup will be introduced in this paragraph. Unlike other SONAR systems that do a ping-wise processing of the receive data, our system processes the data in a frame-wise manner to increase the flexibility in altering the system settings 'mid-ping'.

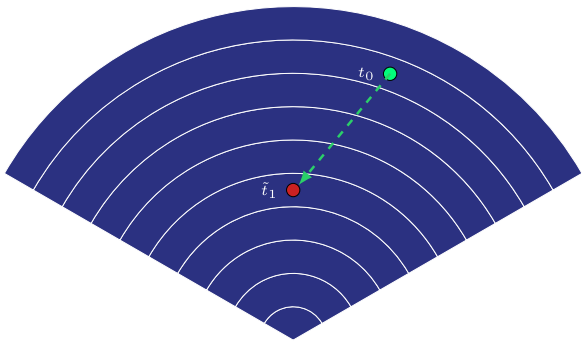

(a) Standard processing: $t_0 < \tilde{t}_1$ and $\tilde{t}_1 = T_{\mathrm{p}} + t_0 = t_3$.

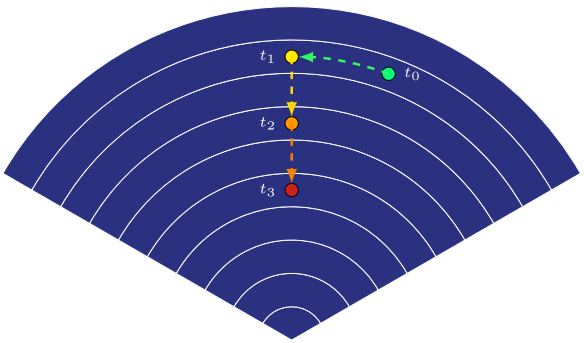

(b) Orthogonal ping MIMO processing: $t_0 < t_1 < t_2 < t_3$ with $t_1 = T_{\mathrm{P,MP}} + t_0$, $t_2 = 2\,T_{\mathrm{P,MP}} + t_0$ and $t_3 = 3\,T_{\mathrm{P,MP}} + t_0 = T_{\mathrm{p}} + t_0 = \tilde{t}_1$.

FIGURE 4 The ping period is chosen to be $T_p = 3\ T_{P,MP}$. While orthogonal ping MIMO processing can resolve the target movement pattern as shown on the right graphic, a standard SONAR processing—no matter whether MIMO or SIMO is used—estimates a movement as shown on the left graphic

Therefore, targets in proximity of the system's location can be evaluated with higher temporal resolution, and the response-time of the SONAR is reduced. Because of the advantages that arise with the use of orthogonal signals (also between different pings), the time between pings can be reduced, while listening time, and hence the observed range, remains constant. In addition, different listening times for different pings are possible in our system. Those systems are in general referred to as *cognitive* if environmental data is additionally considered.

In addition to these, at least in theory, exclusively positive effects caused by the possibility of fast consecutive orthogonal pings that do not interfere with each other, there are also disadvantages in cases of practical application. On the one hand, the cross-correlation of imperfect orthogonal sequences causes disturbances, and on the other hand, clutter is increased because of the higher power emitted into the channel. Nevertheless, it is expected that the operational advantages will outweigh the disadvantages.

The application of frame-based processing enables the system to process receive signals more 'continuously'. That means processing is done in batches defined by the length of the frameshift in samples (L_F) of the system instead of the ping-length in samples (L_P). This will greatly reduce the time of detection for potential targets TTD in the proximity of the SONAR platform and is shown in Figure 5.

This mechanism can be explained with a simple example. Let us assume a system with a sample rate of $f_S = 192$ kHz, a frame length of $L_F = 8192$ samples, and a ping period $T_p = 1$s. The frame length corresponds to a time of $L_F/f_s = 0.043$s. Comparing the length of a frame with the length of a ping illustrates the superiority of frame-based processing in terms of detection time. However, it must be ensured that for all parts of the SONAR system, frame-based processing structures are used. Tracking algorithms, for example, must update the tracks in a sequential (ordered) manner. In each frame, a couple of potential objects within specific range cells are detected, and the corresponding tracks must be updated. If the updated tracks lead to a reaction, for example, a course correction or an alert, this reaction must be done immediately even if the ping period is not yet finished. The power of frame-based processing can be harnessed even more with a cognitive system.

A cognitive system where a main control unit alters parameters of algorithms based on knowledge gained from previous measurements benefits highly from the differences of frame-based processing over ping-based processing as introduced in [15] and proposed, for example, in [14, 16, 17]. It needs to be mentioned that the reaction time of those systems is confined by the delay introduced by utilized filter banks, although this limitation is not crucial in most applications as it is negligible for increasing ranges.

The MIMO receive processing types are compared for both methods in the following. The transmit side processing is neglected, as it is the same for all MIMO realizations, and is, besides the missing transmit beamformer, equal to that of a SIMO system.

To conduct a fair comparison between the different MIMO approaches and SIMO, where the received processing needs to be repeated based on the number of transmit beams that are necessary to illuminate an identical area to MIMO, a minimum achievable angular resolution, and as such, a meaningful number of beams N_B, needs to be defined as a requirement. For this purpose, the Rayleigh criterion is often used [18]. Given a ULA, the minimum possible beamwidth for filter-and-sum beamforming is achieved for the rectangular windowing assumed in the following. Under these considerations, the Rayleigh criterion for the single slit holds and is a sufficient approximation for the following considerations. It is defined by

$$\sin(\theta_R) = \frac{\lambda}{d}, \tag{16}$$

with $d = d_{\max} = \max\{(N_{Tx} - 1)\ d_{El,Tx},\ (N_{Rx} - 1)\ d_{El,Rx}\}$ and λ the wavelength according to the array design frequency. From this, a minimum reasonable mutual angular resolution in radians for transmit and receive beamforming follows:

$$\theta_{R,\,\min} = \arcsin\left(\frac{\lambda}{\max\{(N_{Tx} - 1)\, d_{El,Tx},\ (N_{Rx} - 1)\, d_{El,Rx}\}}\right). \tag{17}$$

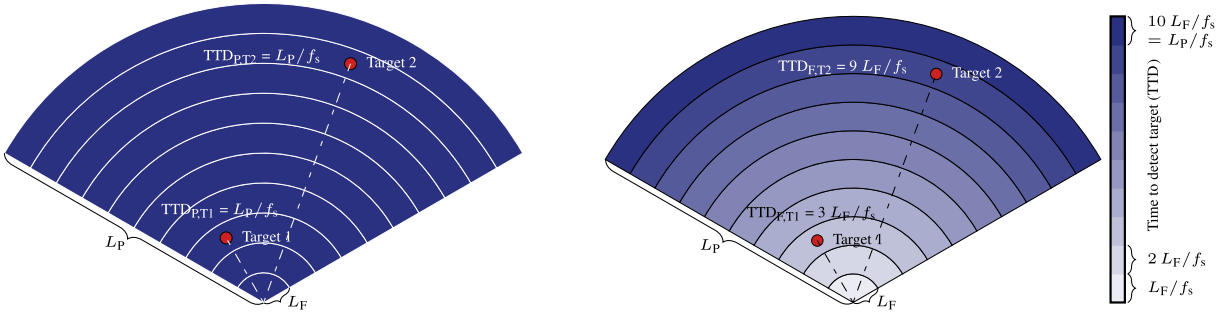

(a) Ping-based processing. **(b)** Frame-based processing.

FIGURE 5 Minimum time necessary to detect a target TTD for ping-based and frame-based processing. For visualization purposes, the ping-length is chosen to be $L_P = 10L_F$. The propagation path to the target and the reflection to the receiver are considered in the shown detection times

A higher resolution for beamforming is not necessary in all cases, as it leads to interpolation and should therefore not be further investigated. Note that computational complexity can be further reduced when the minimum angle is calculated for transmit and receive side independently. A maximum number of processed beams in case of a fan-width of ψ can be postulated:

$$N_{\mathrm{B}} = \frac{\psi}{\theta_{\mathrm{R}}} = \frac{\psi}{\arcsin\left(\frac{\lambda}{\max\{(N_{\mathrm{Tx}}-1)\, d_{\mathrm{El,Tx}},\, (N_{\mathrm{Rx}}-1)\, d_{\mathrm{El,Rx}}\}}\right)}. \tag{18}$$

In the case where $N_{\mathrm{B}} \notin \mathbb{N}$, it needs to be rounded and $\theta_{\mathrm{R,min}}$ updated accordingly. The above presented formula holds for $\max\{N_{\mathrm{Tx}} \;\; N_{\mathrm{Rx}}\}$; otherwise, the number of beams is set to $N_{\mathrm{B}} = 1$ because beamforming is not possible.

Considering the equations of the utilized algorithms introduced in Section 2.2, assuming frequency domain processing and by defining the complexity of one complex multiplication as four floating-point multiplications and two floating-point additions and one complex addition as two floating-point additions, the following complexities can be derived:

- *Beamforming* for N_B directions over N elements yields $4N\; N_{\mathrm{B}}\; N_{\mathrm{FFT}}$ multiplications and $4\left(N-\frac{1}{2}\right) N_{\mathrm{B}}\, N_{\mathrm{FFT}}$ additions per frame or ping, where $N_{FFT} = N_{FFT,F}$ (frame-based processing) or $N_{FFT} = N_{FFT,P}$ (ping-based processing) holds, respectively.
- *Matched filtering* (per ping and signal) for an FFT length of $N_{FFT,P}$ yields $4N_{\mathrm{FFT,P}}$ multiplications and $2N_{\mathrm{FFT,P}}$ additions.
- *Matched filtering* (per frame and signal) for an FFT length of $N_{FFT,F}$ yields $4L_{\mathrm{S,F}}\; N_{\mathrm{FFT,F}}$ multiplications and the following additions:

$$4\left(L_{\mathrm{S,F}} - \frac{1}{2}\right) N_{\mathrm{FFT,F}}$$

Furthermore, let the FFT size for ping-based processing be defined by $N_{\mathrm{FFT,P}} = 2^{\lceil \log_2(L_{\mathrm{P}}) \rceil}$. The FFT size for frame-based processing $N_{\mathrm{FFT,F}}$ is a variable parameter, and the frame length in samples is defined by $L_{\mathrm{F}} = N_{\mathrm{FFT,F}}$. The number of frames in one ping including potential zero padding is calculated as

$$N_{\mathrm{F,P}} = \left\lceil \frac{L_{\mathrm{P}}}{L_{\mathrm{F}}} \right\rceil \tag{19}$$

From the signal length (L_{S}), the signal length in frames can be derived by

$$L_{\mathrm{S,F}} = \left\lceil \frac{L_{\mathrm{S}}}{L_{\mathrm{F}}} \right\rceil \tag{20}$$

From this, one can conclude that the number of calculations for ping-based processing differs by a factor of $N_{\mathrm{FFT,P}}/(N_{\mathrm{FFT,F}} \;\; N_{\mathrm{F,P}})$over frame-based processing where in general, $N_{\mathrm{FFT,P}} \geq N_{\mathrm{FFT,F}}$ holds. Under these considerations, the complexities for the different system setups as depicted in Figure 2 can be derived as shown in Table 1 and named $N_{\mathrm{add.}}$ and $N_{\mathrm{mul.}}$. To do a fair comparison between the two modes, the formulae for ping-based and frame-based processing presented in Table 1 per frequency bin need to be multiplied by an additional factor of

$$N_{\mathrm{FFT,P}} \tag{21}$$

or

$$N_{\mathrm{FFT,F}}\, N_{\mathrm{F,P}} \tag{22}$$

respectively. This is shown in the following equations for frame-based and ping-based processing, respectively, where A_{add} and A_{mul} describe the complexities of the FFTs and will be introduced later in this section:

$$N_{\mathrm{tot.\ add.,frame}} = N_{\mathrm{add.,frame}}\, N_{\mathrm{FFT,F}}\, N_{\mathrm{F,P}} + A_{\mathrm{add}}\left(C_{\mathrm{M}} = N_{\mathrm{F,P}}\right) \tag{23}$$

$$N_{\mathrm{tot.\ mul.,frame}} = N_{\mathrm{mul.,frame}}\, N_{\mathrm{FFT,F}} + A_{\mathrm{mul}}\, N_{\mathrm{F,P}}\left(C_{\mathrm{M}} = N_{\mathrm{F,P}}\right) \tag{24}$$

$$N_{\mathrm{tot.\ add.,ping}} = N_{\mathrm{add.,ping}}\, N_{\mathrm{FFT,P}} + A_{\mathrm{add}}(C_{\mathrm{M}} = 1) \tag{25}$$

$$N_{\mathrm{tot.\ mul.,ping}} = N_{\mathrm{mul.,ping}}\, N_{\mathrm{FFT,P}} + A_{\mathrm{mul}}(C_{\mathrm{M}} = 1) \tag{26}$$

Now, the two approaches are comparable in their complexities for processing one ping for all frequencies. It should be mentioned that in general, just a subset of frequencies is calculated (this is also inherent for baseband processing). This can be accounted for by replacing $N_{\mathrm{FFT,P}}$ or $N_{\mathrm{FFT,F}}$ by $\frac{\mathrm{Bw}}{f_s}\, N_{\mathrm{FFT,P}}$ or $\frac{\mathrm{Bw}}{f_s}\, N_{\mathrm{FFT,F}}$, respectively. It is obvious that all complexities are equally decreased by a factor of $\frac{\mathrm{Bw}}{f_s}$, and the relative outcome is not changed. Bw denotes the bandwidth used by the system.

In addition, the complexity of FFT realizations can be described by $\mathcal{O}(N \log_2 N)$, and as such, increases non-linearly with the length of the FFT. To account for this, penalizing terms defining the increase in computations for both frame-based and ping-based processing need to be calculated and later applied. For the following considerations, the terms presented in [19] are adapted to FFT + IFFT calculations for all input (N_{Rx}) and output (N_{B}) channels and are added to the number of multiplications and additions to penalize the ping-based processing method over frame-based processing:

TABLE 1 Complexities of processing for different permutations of multiple-input multiple-output algorithms in the processing sequence and SIMO (floating-point multiplications (mult.)/additions (add.)) per ping/frame and bin. Complexities are given as a percentage for less optimized straight forward applications of MIMO (b) and (c) and for a system as defined in Section 4, that is, for $f_s = 192$ kHz, $T_S = 0.05$ s and hence $L_S = 9600$ samples, $L_F = 2048$ samples and $N_{FFT} = N_{FFT,F} = 2048$ (for frame-based processing), or $L_P = 192,000$ samples and $N_{FFT} = N_{FFT,P} = L_P$ (for ping-based processing). Additionally, the number of transmit and receive elements is assumed to be $N_{Tx} = 32$ and $N_{Rx} = 32$, respectively. To compare both processing modes the number of bins per ping Equation (21) or Equation (22) and the complexity of the FFTs Equation (27) and Equation (28) need to be considered additionally. This has been done for the complexities given in the last column to have a fair comparison between the different modes

Permutations of algorithms		Ping-based processing	Frame-based processing	Complexity Ping/frame
(a) $Bf_{Rx.} \rightarrow MF \rightarrow Bf_{Tx.}$	$N_{mul.}$	$4(N_{Rx} + 2N_{Tx})\,N_B$	$4\big(N_{Rx} + N_{Tx} + N_{Tx}\,L_{S,F}\big)\,N_B$	8.92 %/11.67 %
	$N_{add.}$	$4\big(N_{Rx} + \frac{3}{2}\,N_{Tx} - 1\big)\,N_B$	$4\big(\big(N_{Rx} - \frac{1}{2}\big) + \big(N_{Tx} - \frac{1}{2}\big)\big)$	7.53 %/10.37 %
			$+ N_{Tx}\,\big(L_{S,F} - \frac{1}{2}\big)\big)\,N_B$	
(b) $MF \rightarrow Bf_{Rx.} \rightarrow Bf_{Tx.}$	$N_{mul.}$	$4(N_{Rx} + N_{Rx}\,N_B + N_B)\,N_{Tx}$	$4\big(N_{Rx}\,L_{S,F} + N_{Rx}\,N_B + N_B\big)\,N_{Tx}$	100 %/100 %
	$N_{add.}$	$2\big(N_{Rx}\,N_{Tx} + 2\big(N_{Rx} - \frac{1}{2}\big)\,N_{Tx}\,N_B$	$4\big(N_{Rx}\,N_{Tx}\,\big(L_{S,F} - \frac{1}{2}\big)$	100 %/100 %
		$+ 2\big(N_{Tx} - \frac{1}{2}\big)\,N_B\big)$	$+ \big(N_{Rx} - \frac{1}{2}\big)\,N_{Tx}\,N_B + \big(N_{Tx} - \frac{1}{2}\big)N_B\big)$	
(c) $MF \rightarrow Bf_{Tx.} \rightarrow Bf_{Rx.}$	$N_{mul.}$	$4(N_{Tx} + N_{Tx}\,N_B + N_B)\,N_{Rx}$	$4\big(N_{Tx}\,L_{S,F} + N_{Tx}\,N_B + N_B\big)\,N_{Rx}$	100 %/100 %
	$N_{add.}$	$2\big(N_{Rx}\,N_{Tx} + 2\big(N_{Tx} - \frac{1}{2}\big)\,N_{Rx}\,N_B$	$4\big(N_{Rx}\,N_{Tx}\,\big(L_{S,F} - \frac{1}{2}\big) + \big(N_{Tx} - \frac{1}{2}\big)\,N_{Rx}\,N_B$	100 %/100 %
		$+ 2\big(N_{Rx} - \frac{1}{2}\big)\,N_B\big)$	$+ \big(N_{Rx} - \frac{1}{2}\big)\,N_B\big)$	
(d) $MF \rightarrow Bf_{Comb.}$	$N_{mul.}$	$4(1 + N_B)\,N_{Rx}\,N_{Tx}$	$4\big(L_{S,F} + N_B\big)\,N_{Rx}\,N_{Tx}$	97.03 %/97.08 %
	$N_{add.}$	$2\big(N_{Rx}\,N_{Tx} + 2\big(N_{Rx}\,N_{Tx} - \frac{1}{2}\big)\,N_B\big)$	$4\big(N_{Rx}\,N_{Tx}\,\big(L_{S,F} - \frac{1}{2}\big) + \big(N_{Rx}\,N_{Tx} - \frac{1}{2}\big)\,N_B\big)$	98.48 %/98.51 %
(e) MIMO-MF $\rightarrow Bf_{Rx.}$	$N_{mul.}$	$8\,N_{Rx}\,N_B$	$4\,N_{Rx}\,N_B\,\big(L_{S,F} + 1\big)$	5.95 %/8.75 %
	$N_{add.}$	$6\big(N_{Rx} - \frac{1}{3}\big)\,N_B$	$4\big(N_{Rx}\,\big(L_{S,F} + \frac{1}{2}\big) - \frac{1}{2}\big)\,N_B$	4.52 %/7.43 %
(f) $Bf_{Rx.} \rightarrow$ MIMO-MF	$N_{mul.}$	$4(N_{Rx} + 1)\,N_B$	$4\big(N_{Rx} + L_{S,F}\big)\,N_B$	3.07 %/3.1 %
	$N_{add.}$	$4\,N_{Rx}\,N_B$	$4\big(N_{Rx} + L_{S,F} - 1\big)\,N_B$	3.05 %/3.08 %
(i) SIMO: $Bf_{Rx.} \rightarrow$ MF	$N_{mul.}$	$(4N_{Tx} + 4N_{Rx} + 4)N_B$	$\big(4N_{Tx} + 4N_{Rx} + 4L_{S,F}\big)N_B$	6.04 %/6.02 %
	$N_{add.}$	$(2N_{Tx} + 4\big(N_{Rx} - \frac{1}{2}\big) + 2)N_B$	$\big(2N_{Tx} + 4\big(N_{Rx} - \frac{1}{2}\big) + 4\big(L_{S,F} - \frac{1}{2}\big)\big)N_B$	4.57 %/4.58 %
(ii) SIMO: $MF \rightarrow Bf_{Rx.}$	$N_{mul.}$	$(4N_{Tx} + 4N_{Rx} + 4N_{Rx})N_B$	$\big(4N_{Tx} + 4L_{S,F}N_{Rx} + 4N_{Rx}\big)N_B$	8.92 %/11.67 %
	$N_{add.}$	$\big(2N_{Tx} + 2N_{Rx} + 4\big(N_{Rx} - \frac{1}{2}\big)\big)N_B$	$\big(2N_{Tx} + 4\big(L_{S,F} - 1/2\big)N_{Rx} + 4(N_{Rx} - 1/2)\big)N_B$	6.05 %/8.93 %

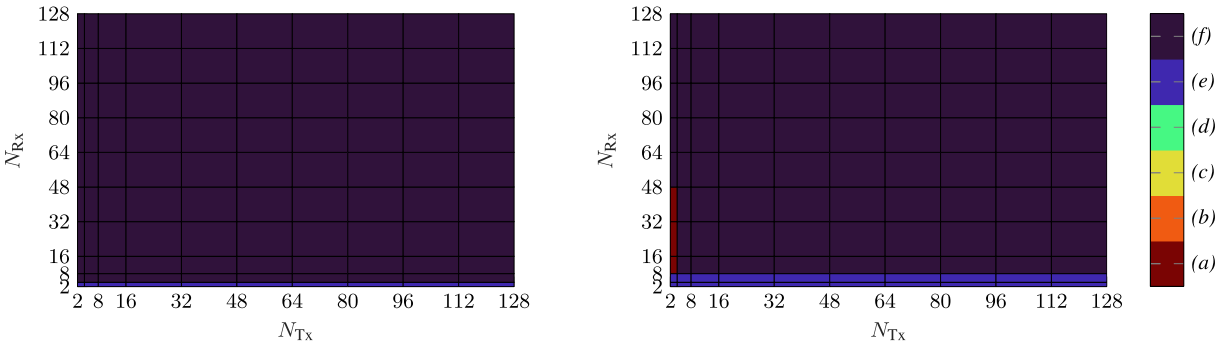

(a) Lowest complexity with respect to multiplications.

(b) Lowest complexity with respect to additions.

FIGURE 6 Algorithm with lowest complexity for ideal frame length ($L_{F,opt}$) and variable transmitter and receiver number. The algorithms (a) to (f) are colour-coded from red (a) to blue (f). The map entry for each setting is marked according to the winner algorithms colour

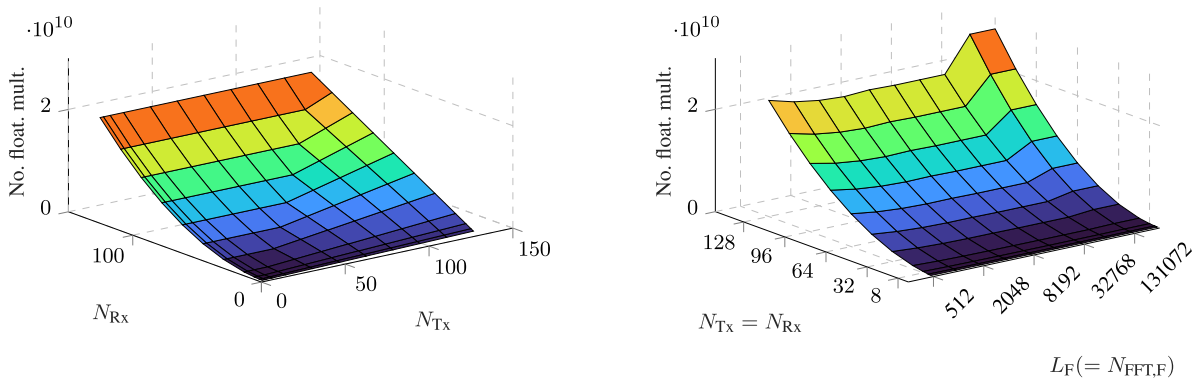

(a) Complexities for different transmitter and receiver numbers at a fixed, optimal FFT length ($N_{FFT,F} = L_{F,opt}$).

(b) Complexities for $N_{Tx} = N_{Rx}$ but variable frame length (and FFT length).

FIGURE 7 Complexities for different settings of variant (f) for frame-based processing. The colour map shows the complexity depicted on the *z*-axis colour-coded from blue (low) to red (high)

$$A_{mul} = 3\left(\log_4(N_{FFT}) - 1\right)(N_{Rx} + N_B)\, C_M \tag{27}$$

and

$$A_{add} = 8\log_4(N_{FFT})\,(N_{Rx} + N_B)\, C_M \tag{28}$$

respectively. The value C_M considers the different number of processing steps for ping-based and frame-based processing and takes values from $C_M = 1$ and $C_M = N_{F,P}$, respectively.

The computational complexity for each presented permutation of the individual algorithms is listed in Table 1 and visualized in Figure 8a,b for an exemplary high-frequency SONAR system based on our prototype. In the case of SIMO, the necessity of transmitting several pings to illuminate the same area as MIMO processing does with one ping is accounted for by multiplying the complexity of the receive side processing by a factor of N_B. Considering this and the fact that matched filtering and receive beamforming can be interchanged, complexities for frame-based and ping-based processing are given in Table 1 as well.

The system runs with a sample rate of $f_s = 192$ kHz. The ping period in samples is set to $L_P = 1\ \text{s} \cdot f_s$, and the signal length in samples to $L_S = 0.05\ \text{s} \cdot f_s$. Furthermore, the number of transmitter elements equals the number of receive elements with $N_{Tx} = N_{Rx} \in \{2, 3, \ldots, 128\}$. The number of beams N_B is calculated according to Equation (18), and both FFT length for frame-based processing and the frameshift take values of $N_{FFT,F} = L_F = 2^C$ with $C \in \{9, 10, \ldots, \lceil \log_2(L_P) \rceil\}$.

When considering the best algorithm in terms of the number of multiplications per setting (see Figure 6a) with variable numbers of transmitters and receivers (and thus also numbers of beams, see Equation (18)), it also becomes clear that variant (f) is the less complex algorithm apart from receiver number two. Here the second structure (e) presented by us is superior.

When considering the necessary additions (see Figure 6b) to calculate the algorithm, (e) is ahead until the number of receiver elements reaches eight. With only two transmitting elements and a receiver number of 8–48 elements, the direct MIMO implementation (a) wins in terms of additions. However, because only two transmitters could be used here and the number of multiplications for variant (f), for example, is lower,

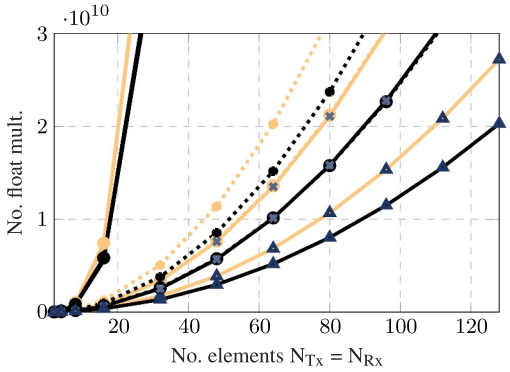

(a) Complexity of all processing types for fixed $L_P = f_s$, $N_{FFT,P} = 2^{\lceil \log_2(L_P) \rceil}$ and $L_F = L_{F,opt}$ and variable number of transmitter and receiver elements where $N_{Tx} = N_{Rx}$.

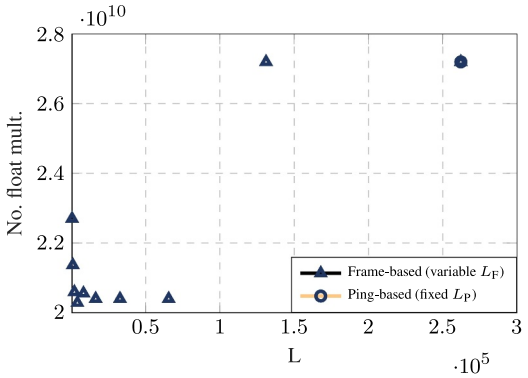

(b) Complexity of processing chain *(f)* (receive beamforming / MIMO matched filtering) for $N_{Tx} = N_{Rx} = 128$, $L_P = f_s\,1\,s^{-1}$ = constant and variable L_F for frame- and ping-based processing.

FIGURE 8 Comparison of computational complexity by reference to floating-point multiplications for different proposed processing chains and ping-based (black) versus frame-based processing (yellow). The number of beams is chosen adaptively according to the Rayleigh criterion, $f_s = 192$ *kHz*, $L_S = f_s \cdot 0.05\,s^{-1}$ *and* $L_P = f_s \cdot 1\,s^{-1}$. The different processing types are assigned as follows for frame-based processing: SIMO like (i) (•-●-•)/SIMO like (ii) (•-✱-•)/MIMO (a) (•-✚-•)/MIMO (b) (—✱—)/MIMO (c) (- ● -)/MIMO (d) (——)/MIMO (e) (—✖—)/MIMO (f) (—▲—). Ping-based processing is assigned accordingly but in yellow

the advantage is evened out again. Figure 7 illustrates the number of multiplications for variant (f) to clarify the dependence of different parametrizations on the complexity of this variant. This motivates why further comparisons can be limited to a restricted set of parametrizations of the algorithm. On the one hand, this is done depending on sender and receiver with ideal frame length, and on the other hand, for $N_{Tx} = N_{Rx}$ but variable frame lengths. Looking at Figure 7a, it can be observed that N_{Tx} has no influence on the complexity as long as $N_{Tx} < N_{Rx}$ is valid. This is obvious, because on the one hand, the matched filter prototypes are calculated beforehand, and on the other hand, they are correlated with N_B matched filter input signals. The number of beams (N_B) in turn depends on $\max(N_{Tx}, N_{Rx})$ according to Equation (18). Based on the findings from Figures 6 and 7, for a better presentation and for a clearer comparison, we will limit ourselves to $N_{Rx} = N_{Tx}$ (Figure 8) when considering the optimal frame length.

Looking at Figure 8a, for a small number of transmitter and receiver elements (i.e. eight and less), the complexity of the different MIMO realizations is merely the same. With an increasing number of elements ($N_{Tx} = N_{Rx} \geq 8$), however, the application of a more sophisticated permutation of the different receive side algorithms has a noticeable impact. Comparing the number of additions and multiplications, it can be observed that the new approach of including the receive side transmit beamforming into the matched filter, especially setup (f), outperforms all the other realizations with regard to computational complexity. It should be noted that the impact of computational savings for this approach increases for higher pulse lengths and greater ping periods, and this becomes obvious by looking on Table 1. Furthermore, it can be observed that a minimum complexity for frame-based processing is achieved at a FFT length and frame length of

$$L_{F,opt.} = N_{FFT} = 2^{\lceil \log_2(L_S) \rceil}. \tag{29}$$

This shows that frame-based processing outperforms ping-based processing not only in flexibility but also in computational complexity if an appropriate frame length (L_F) is used. Another important observation is that there is no decisive difference in complexity between SIMO and MIMO processing if permutation (f) is chosen. Please note that the calculations of the SIMO complexities also consider the process of transmit beamforming to conduct a fair comparison. In fact, for a truly fair comparison, it would be necessary to perform the above-mentioned processing N_B times to illuminate the same area as the MIMO processing does.

However, if the transmit processing of SIMO is not considered, all terms containing the number of transmit elements N_{Tx} vanish. The complexity of SIMO processing (ii) becomes identical to that of MIMO (e). The same holds for (i) and (f). This is obvious as no dedicated transmit beamforming is calculated in those MIMO variants because it is integrated into the matched filtering process.

To give a classification of the complexity of the presented algorithms in practical implementation on modern PC systems, the values for billion floating-point operations per second (GFLOPS) are examined in the following. Assume for simplicity that an addition is seen as one floating-point operation and so does a multiplication as well—although some modern CPUs may be capable of handling several instructions per cycle. Hence, additions and multiplications as defined in Equations (23)–(26) can be summed up and referenced to instructions per second by

$$C_{GFLOPS} = f_s / L_P \cdot 10^{-9}, \tag{30}$$

to calculate a value for GFLOPS:

$$N_{GFLOPS,frame} = (N_{tot.\ add.,frame} + N_{tot.\ mul.,frame})\, C_{GFLOPS}, \tag{31}$$

TABLE 2 Values for billion floating-point operations per second for the complexities presented in Table 1 and calculated by Equations (31) and (32)

Permutations of algorithms	GFLOPS (ping)	GFLOPS (frame)
(a) $\mathrm{Bf}_{\mathrm{Rx.}} \rightarrow \mathrm{MF} \rightarrow \mathrm{Bf}_{\mathrm{Tx.}}$	9.2	9.44
(b) $\mathrm{MF} \rightarrow \mathrm{Bf}_{\mathrm{Rx.}} \rightarrow \mathrm{Bf}_{\mathrm{Tx.}}$	111.99	85.6
(c) $\mathrm{MF} \rightarrow \mathrm{Bf}_{\mathrm{Tx.}} \rightarrow \mathrm{Bf}_{\mathrm{Rx.}}$	111.99	85.6
(d) $\mathrm{MF} \rightarrow \mathrm{Bf}_{\mathrm{Comb.}}$	109.46	83.7
(e) $\mathrm{MIMO\text{-}MF} \rightarrow \mathrm{Bf}_{\mathrm{Rx.}}$	5.87	6.93
(f) $\mathrm{Bf}_{\mathrm{Rx.}} \rightarrow \mathrm{MIMO\text{-}MF}$	3.42	2.65
(i) SIMO: $\mathrm{Bf}_{\mathrm{Rx.}} \rightarrow \mathrm{MF}$	5.95	4.54
(ii) SIMO: $\mathrm{MF} \rightarrow \mathrm{Bf}_{\mathrm{Rx.}}$	8.4	8.83

$$N_{\mathrm{GFLOPS,ping}} = \left(N_{\mathrm{tot.\ add.,ping}} + N_{\mathrm{tot.\ mul.,ping}}\right) C_{\mathrm{GFLOPS}}. \tag{32}$$

The results are depicted in Table 2. Although modern CPUs like 8th+ generation Intel Core-i or AMD Ryzen processors can easily reach 500–800 GFLOPS, the MIMO algorithm is not the only processing done in a modern SONAR or RADAR system. In view of this result, it is again clear how much permutation (f) exceeds the other permutations of the algorithm, as it occupies less than 1% of the processing power of modern high-end CPUs.

5 | SIMULATION RESULTS

The different proposed permutations of the algorithms in the processing sequence have been simulated in terms of computational complexity and the system's output signals, which should ideally be the same for the different permutations.

The simulations were made for frame-based processing given a sample rate of $f_s = 192$ kHz, a frameshift of $L_F = 2048$ samples, an FFT length of $N_{FFT} = 2048$, and a ping period of $T_p = 1$ s. The transmitted signals are orthogonal signals based on non-deterministic (noise-coded) sequences with a pulse length of $T_S = 0.05$ s, a centre frequency of $f_c = 60$ kHz, and a bandwidth of $\mathrm{Bw} = 15$ kHz.

The SONAR system consisted of a monostatic setup with $N_{Tx} = 32$ transmit elements and $N_{Rx} = 32$ receive elements. Both were arranged on a ULA with a $\lambda/2$-spacing according to the signal's centre frequency f_c. The targets are located at a distance of 35 m at $\theta = \pm 45°$.

This setup has been chosen to be able to compare the results with measurements that we will perform with our projector array that is depicted in Figure 1.

Looking at Figure 9a, the previous results in connection with computational complexity, are confirmed qualitatively. The necessity of an intelligent permutation of the system's subalgorithms and the superiority of the proposed matched filter method and especially permutation (f) is emphasized again.

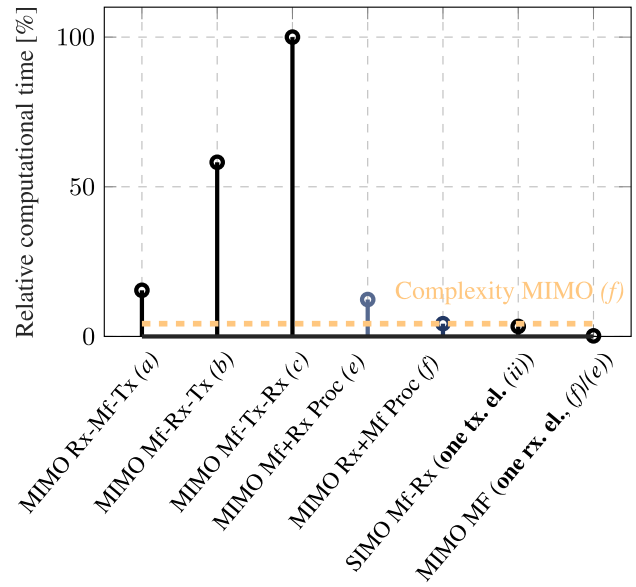

(a) Computational time of simulations relative to type *(b)*.

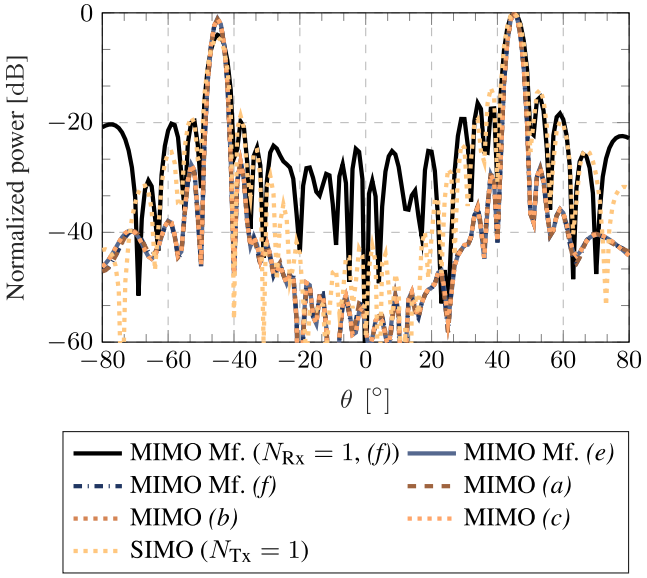

(b) SONAR system output at range of targets.

FIGURE 9 Results of simple simulation for targets in distance 35 m at angles $\theta = \pm 45°$ for all presented arrangements of receive processing algorithms. The SONAR system's settings for which the simulation was conducted are depicted in Table 1

To classify the graphics shown for the SONAR system's output for different setups, the results of MIMO in comparison with SIMO will be analysed briefly without in-depth introductions and explanations. For this, terms such as 'virtual array' or 'co-array' (CA) are assumed to be known. Again, reference is made to existing literature, for example, [8, 10, 11].

Given our simulation setup, the resulting CA will obviously consist of several overlapping elements that induce an

(a) GUI for development use.

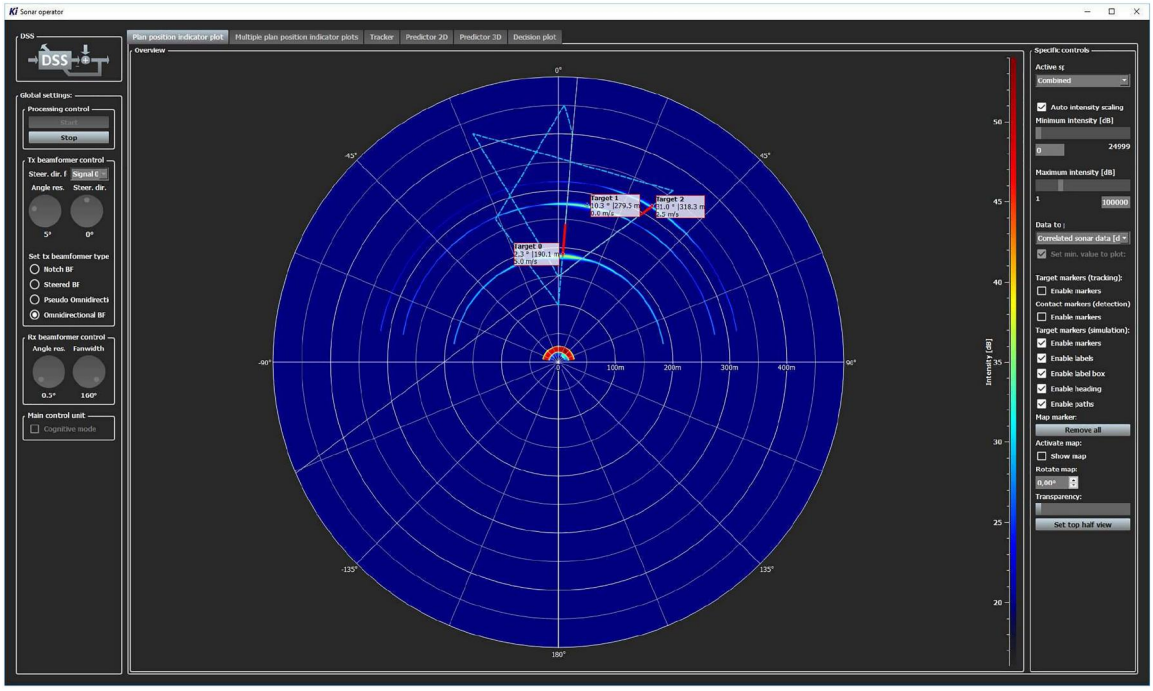

(b) GUI for SONAR operator.

FIGURE 10 Graphical user interface of our real-time processing unit. A multiple-input multiple-output system with 16 projectors and 16 hydrophones operating at 192 kHz can be computed in real-time using permutation (f)

additional triangular tapering. The number of unique elements of the CA results in $N_{\mathrm{CA}} = N_{\mathrm{Tx}} + N_{\mathrm{Rx}} - 1 = 31$. This is clearly visible in Figure 9b.

The higher number of unique elements (31 instead of 16) leads to a narrower main lobe in comparison to SIMO (for non-overlapping, unique element positions, this effect is

maximized). The suppression of side lobes, which can be observed in Figure 9b, results from an additional tapering (in this case triangular) due to the overlapping of elements (non-unique elements) in the CA. All MIMO realizations produce identical output signals. This was expected and confirmed by the simulations.

In addition, a MIMO system according to arrangement (f) with $N_{\mathrm{Tx}} = 16$ transmit elements and $N_{\mathrm{Rx}} = 1$ receive elements was simulated. In comparison with SIMO for $N_{\mathrm{Tx}} = 1$ and $N_{\mathrm{Rx}} = 16$ and the same overall antenna geometry an almost identical output signal is obtained, see Figure 9b lines (——) and (·····) for MIMO and SIMO, respectively.

The differences in the area of the side lobes, which peak at values smaller than −30 dB, can be explained by the signals used. Since the signals are not perfectly orthogonal to each other, a cross-correlation is obtained that deviates from zero. This leads to a fixed beamforming in broadside direction, and hence the results of MIMO signal processing differ slightly from those of SIMO.

This detail represents another important aspect of MIMO SONAR systems—a design of matched orthogonal signals. A MIMO SONAR adapted signal design has been done, for example, by [20, 21].

This area will be investigated more closely in the future, as signal design specifically catering the needs of MIMO SONAR systems is rare. In addition, the simulation presented will be verified by measurements under real conditions. Simulations showing the basic functionality of MIMO have been done before for RADAR applications, and the results are promising [22]. Therefore, the proposed MIMO arrangement (f) was implemented in a real-time system that contains a fully working SONAR system (including all relevant algorithms (beamforming, matched filtering, detection, tracking and a presentation via a graphical user interface). The user interface is depicted in Figure 10. In the future, the simulation results presented here will be compared with real measurements at sea.

6 | CONCLUSION

The fundamentals of MIMO signal processing were summarized. The underlying channel model was revised and the influence of orthogonal signals on transmit and receive processing was considered. Furthermore, the influence of non-perfect orthogonal signals was discussed, and the importance of an adapted signal design was emphasized. This was achieved based on theory as well as simulations.

Based on these considerations, different arrangements of the receive processing algorithms were presented and examined for the computational load and equivalence of the output signals. In this context, a novel application of the matched filter was presented and investigated based on simulations.

It was shown that the arrangement of the algorithms has a great influence on the real-time capability of the SONAR system. In addition, the presented MIMO matched filter far exceeds the conventional algorithm for computational load without having an influence on the result of the signal processing chain. Especially, our proposed structure (f) outperforms all others and hence is an important part of creating real-time capable MIMO SONAR systems.

In the future, the simulated results will be verified in practical measurements as stated above. For this purpose, a SONAR signal design adapted to both the MIMO technology and the utilized SONAR system used will be further developed.

ORCID

Thorben Kaak https://orcid.org/0000-0003-4926-0244
Gerhard Schmidt https://orcid.org/0000-0002-6128-4831

REFERENCES

1. Rabideau, D.J., Parker, P.: Ubiquitous mimo multifunction digital array radar. In: The Thirty-Seventh Asilomar Conference on Signals, Systems Computers, vol. 1, pp. 1057–1064. (2003)
2. Forsythe, K.W., Bliss, D.W., Fawcett, G.S.: Multiple-input multiple-output (MIMO) radar: performance issues. In: Conference Record of the Thirty-Eighth Asilomar Conference on Signals, Systems and Computers, vol. 1, pp. 310–315. (2004)
3. Bliss, D.W., Forsythe, K.W.: Multiple-input multiple-output (MIMO) radar and imaging: degrees of freedom and resolution. In: The Thirty-Seventh Asilomar Conference on Signals, Systems Computers. vol. 1, pp. 54–59. (2004)
4. Bekkerman, I., Tabrikian, J.: Target detection and localization using MIMO radars and sonars. IEEE Trans. Signal Process. 54, 3873–3883 (2006)
5. Li, J., Stoica, P.: MIMO radar with colocated antennas. IEEE Signal Process Mag. 24, 106–114 (2007)
6. Fishler, E., et al.: MIMO radar: an idea whose time has comel. In: Proceedings of the 2004 IEEE Radar Conference (IEEE Cat. No.04CH37509), pp. 71–78. (2004)
7. Pailhas, Y., Capus, C., Brown, K.E.: Broadband MIMO Sonar System: A Theoretical and Experimental Approach (2009)
8. Hoctor, R.T., Kassam, S.A.: The unifying role of the coarray in aperture synthesis for coherent and incoherent imaging. Proc. IEEE. 78, 735–752 (1990)
9. Davis, M.: MIMO Radar: Signal Processing, Waveform Design, and Applications to Synthetic Aperture Imaging, PhD thesis. School of Electrical and Computer Engineering Georgia Institute of Technology (2015)
10. Richards, M.A.: Virtual Arrays and Coarrays. Part 1: Phase Centres and Virtual Elements. (2017). http://www.radarsp.com/
11. Richards, M.A.: Virtual arrays and coarrays, part 2: the virtual array. Self published on (Aug 2017). http://www.radarsp.com/
12. Hassanien, A., Vorobyov, S.A.: Transmit/receive beamforming for MIMO radar with colocated antennas. In: 2009 IEEE International Conference on Acoustics, Speech and Signal Processing, pp. 2089–2092. (2009)
13. Hassanien, A., Vorobyov, S.A.: Phased-MIMO radar: a tradeoff between phased-array and MIMO radars. IEEE Trans. Signal Process. 58, 3137–3151 (2010)
14. Claussen, T., et al.: A real-time cognitive-sonar system for diver detection. In: Oceans 2015, pp. 1–9. MTS/IEEE, Washington, DC (2015)
15. Haykin, S.: Cognitive radar: a way of the future. IEEE Signal Process Mag. 23, 30–40 (2006)
16. Claussen, T., Nguyen, V.D.: Real-time cognitive sonar system with target-optimised adaptive signal processing through multi-layer data fusion. In: 2015 IEEE International Conference on Multisensor Fusion and Integration for Intelligent Systems (MFI), pp. 357–361. (2015)
17. Kaak, T., Schmidt, G.: An introduction to real-time cognitive SONAR systems utilising novel MIMO approaches. In: DAGA 2017 Kiel, pp. 48–51. (2017)

18. Aldeman, M., et al.: Effects of array scaling and advanced beamforming on the angular resolution of microphone array systems. In: Berlin Beamforming Conference, vol. 6 (2016)
19. He, S., Torkelson, M.: Design and implementation of a 1024-point pipeline fft processor. In: Proceedings of the IEEE 1998 Custom integrated Circuits Conference (Cat. No.98CH36143), pp. 131–134. (1998)
20. Liu, B.: Orthogonal discrete frequency-coding waveform set design with minimised autocorrelation sidelobes. IEEE Trans. Aero. Electron. Syst. 45, 1650–1657 (2009)
21. Pailhas, Y., Petillot, Y.: Wideband CDMA waveforms for large MIMO sonar systems. In: 2015 Sensor Signal Processing for Defence (SSPD), pp. 1–4. (2015)
22. Robey, F.C., et al.: MIMO radar theory and experimental results. In: Conference Record of the Thirty-Eighth Asilomar Conference on Signals, Systems and Computers, vol. 1, pp. 300–304. (2004)

How to cite this article: Kaak T, Abshagen J, Schmidt G. Real-time capable multiple-input–multiple-output SONAR systems—An algorithmic approach. *IET Radar Sonar Navig*. 2021;1–16. https://doi.org/10.1049/rsn2.12091